Computational Energy Science

Vol. 2, No. 2, p. 54-67, 2025

Original article

# A gradient flow-based robust algorithm for solving a sequence of smallest eigenvalues with applications

Na Peng[1], Jijing Zhao[2], Shuyu Sun[2]*

[1]*School of Mathematical Sciences, Guizhou Normal University, Guiyang 550025, P. R. China*
[2]*School of Mathematical Sciences, Tongji University, Shanghai 200092, P. R. China*

**Keywords:**
Gradient flows
length-preserving
unconditional energy stability
error estimation
existence and uniqueness theorem

**Cited as:**
Peng, N., Zhao, J., Sun, S. A gradient flow-based robust algorithm for solving a sequence of smallest eigenvalues with applications. Computational Energy Science, 2025, 2(2): 54-67.
https://doi.org/10.46690/compes.2025.02.03

**Abstract:**
Eigenvalues are core quantities to connect mathematical operators with practical physical and engineering problems. The computation of eigenvalues (and eigen-vectors) is a fundamental numerical procedure with broad and critical applications across engineering, science, and interdisciplinary fields-especially in problems involving dynamic systems, stability analysis, pattern recognition, and multi-physics coupling. In this paper, we first review a few important application examples of eigenvalues in finite element error estimation, energy engineering, quantum mechanics, and chemical adsorption. Existing eigenvalue solving methods have drawbacks such as sensitivity to initial parameters and for iterative methods, lack of robustness with respect to iterations, for eample, difficulty in balancing the preservation of length and unconditional energy stability at the iteration. In this paper, we present an efficient and robust algorithm for solving the first $m$ eigenvalues problem. It can be extended to both linear and nonlinear problems. This algorithm has several unique advantages. It converges to the first eigenpair or the first $m$ eigenpairs from arbitrary initial guesses. Moreover, its strict length preservation and unconditional energy stability ensure high robustness throughout the computation and maintain stable convergence even when large time steps are employed. We begin by deriving the desired gradient flow equation through the introduction of an extended gradient flow and prove that it possesses the properties of length preservation and energy dissipation, implying that the solutions of our gradient flow equation lies on the Stiefel manifold. Then it is proved that the ordinary differential equation form of this equation has the desired property of existence and uniqueness of a solution. We present an effective algorithm and demonstrate that both its ordinary differential equation and discrete scheme retain length preservation and energy dissipation. Finally, the effectiveness of the algorithm is validated through numerical experiments.

## 1. Introduction

The efficient solution of eigenvalue problems play a crucial role in fields such as quantum mechanics, chemical adsorption, energy engineering, and finite element analysis (Golebiewski and Taylor, 1967; Zheng et al., 2013; Griffiths and Schroeter, 2018). Existing numerical methods can be broadly divided into two categories. The first category consists of classical algebraic iterative algorithms, including the Newton iteration (Kublanovskaya, 1970; Khazanov and Kublanovskaya, 1988; Kressner, 2009), residual inverse iteration (Neumaier, 1985), the inverse power method (Allen and Berry, 2002; Kashiwagi, 2009), the QR algorithm (Francis, 1961, 1962), nonlinear inverse iteration (Unger, 1950), Rayleigh quotient iteration (Kaniel, 1966; Geltner, 1981), Krylov methods (He and Prabhu, 2003), the Lanczos algorithm (Parlett, 1990), the Arnoldi algorithm, and Jacobi-Davidson type methods (Sleijpen et al., 1996; Betcke and Voss, 2004; Botchev et al., 2009), among others. While these methods generally have certain advantages and some of them offer high computational efficiency, they face several challenges in practical applications. For instance, the inverse power method is highly sensitive to the selection of initial shift parameters.

Yandy Scientific Press

*Corresponding author.
*E-mail address*: pengna2526@163.com (N. Peng); 24310052@tongji.edu.cn (J. Zhao); suns@tongji.edu.cn (S. Sun).


Received April 20, 2025; revised May 6, 2025; accepted June 15, 2025; available online June 20, 2025.

The second category is based on optimization methods derived from continuous dynamical systems. One desired numerical property for such methods is to strictly preserve the key geometric and physical properties of the original continuous system at the discrete level (Edelman et al., 1998; Budd and Piggott, 2003). However, many existing algorithms struggle to satisfy both requirements simultaneously. Some fail to ensure that the iterative sequence remains on the Stiefel manifold (i.e., length preserving), leading to numerical solution drift. Others only achieve conditional energy stability, meaning that the energy dissipation property holds only when the time step is sufficiently small, which severely restricts computational efficiency and applicability. Consequently, developing an efficient algorithm that can ensure length preservation and unconditional energy stability remains a challenging yet critical task.

In this paper, we present a robust algorithm for solving the smallest eigenvalue, which can be extended to compute the first $m$ minimum eigenvalues. This algorithm overcomes the drawbacks of traditional methods: it converges to the first eigenpair or the first $m$ eigenpairs from arbitrary initial guesses, and maintains high robustness even with large time steps. Furthermore, the algorithm can be extended to both linear and nonlinear problems. In this paper, we derive a length-preserving and energy-dissipative gradient flow equation and prove the existence and uniqueness of its solutions. Subsequently, we design a discrete scheme that possess these essential properties. The algorithm's effectiveness and accuracy are validated through numerical experiments.

The remaining organization of this paper is organized below. In the next section, we list the specific practical applications of eigenvalues in several fields; In section 3, we present a length-preserving and unconditionally energy-stable algorithm for computing the smallest eigenvalue, together with numerical experiments to verify the efficient of the algorithm. In section 4, we extend the algorithm from the previous section to obtain one for solving the first $m$ smallest eigenvalues, which also possesses the properties of preserving length and energy dissipation. In section 5, conclusions are summarized.

## 2. Application of eigenvalues

It has been discovered that many complex problems are inherently related to eigenvalues. For example: the constant $C$ of finite element error estimation can be computed by reformulating into an eigenvalue problem; in the chemisorption problem, they correlate with adsorption properties in chemisorption through electronic energy levels, enabling predictive models; in quantum mechanics, by transforming complex optimization problems into eigenvalue problems, system stability can be intuitively quantified (Lima, 2002). Next, we first outline the role of eigenvalues in these applications, then analyze in detail the intrinsic connections between eigenvalues and two complex fields (chemical adsorption and quantum mechanics).

### 2.1 The relationship between constant $C$ and eigenvalues in finite element error estimation

In finite element error estimation, $C$ depends on the Poincaré constant (Braess, 2007; Banjai and Boulton, 2021), the Babuška-Aziz constant (Liu and Kikuchi, 2010; Liu and Oishi, 2013), element shapes (Durán et al., 1999; Liu and Kikuchi, 2010; Liu and Oishi, 2013, 2013a; Schilling et al., 2014) and inverse inequalities (Liu and Oishi, 2013), ect. All of which are essentially determined by local and global eigenvalues (Ciarlet, 2002). In addition, it has been found that the constant $C$ has a quantitative relationship with eigenvalues. For example, in elliptic equations, the upper bound of $C$ is determined by the eigenvalues of the operator or matrix. Under the $H^1$-norm, $C \leq \sqrt{\lambda_{K,\max}/\lambda_{K,\min}}$, while under the $L^2$ norm, $C$ is positively correlated with the maximum eigenvalue of the error operator (Ciarlet, 1978, 2002); the Poincaré constant is inversely proportional to the smallest eigenvalue of the domain (a smaller eigenvalue yields a larger constant $C$ and a looser error margin), which may lead to misjudge the accuracy of the solution, especially near singular points. We note that this "quantitative relationship between $C$ and eigenvalues" can also be derived from the differences in $C$ values across different element types, as detailed in Table 1. As observed from the table, the relationship between the eigenvalue distribution of different finite element types and the error constant $C$ in the $H^1$-norm is as follows: the higher the concentration of the eigenvalue distribution and the larger its lower bound, the smaller the corresponding $C$ value. Among these, high-order quadrilateral elements exhibit the optimal eigenvalue distribution and the smallest $C$ value, while non-conforming low-order elements show the worst eigenvalue distribution and the largest $C$ value. Additionally, Liu and Kikuchi (2010) indicated that element distortion causes the smallest eigenvalue of the stiffness matrix to approach 0 and $C$ to approach infinity.

### 2.2 Application of eigenvalues in energy engineering

Research has demonstrated that in energy engineering, transforming complex optimization problems into eigenvalue problems offers several advantages: enabling intuitive quantification of system stability (Lima, 2002), effective simplification of high-dimensional complex systems, advance prediction of fault boundaries (Harne, 2012), support for multi-objective optimization design, and compatibility with mainstream engineering tools (Auchmuty, 1989; Lima, 2002). These benefits highlight the significance of eigenvalue methods in energy engineering. Among them, the relevant theoretical methods for transforming complex optimization problems into eigenvalue problems include variational principles (Auchmuty, 1989; Auchmuty and Rivas, 2015), Rayleigh quotient theory (Canfield, 1993), and semidefinite programming relaxation methods (Helmberg and Rendl, 2000; Achtziger and Kočvara, 2008).

For instance, in the small-signal stability-constrained optimal power flow (SSSC-OPF) problem, the stability of the system is entirely determined by the eigenvalues of the state matrix (Gupta et al., 2019; Kerdphol et al., 2021). The system is asymptotically stable when all eigenvalues have negative

**Table 1**. Error constants $C$ and eigenvalue distributions of different finite elements.

| Element type | $C$ ($H^1$-norm) | Eigenvalue range | Reference |
|---|---|---|---|
| Linear triangular (conforming) | 3.82 | 0.12 $\sim$ 2.35 | Brenner, 2008 |
| Quadratic triangular (conforming) | 1.48 | 0.85 $\sim$ 1.92 | Quarteroni and Valli, 2008 |
| Linear quadrilateral (conforming) | 2.55 | 0.65 $\sim$ 2.81 | Ciarlet, 1978 |
| Quadratic quadrilateral (conforming) | 1.12 | 1.02 $\sim$ 1.75 | Quarteroni and Valli, 2008 |
| Linear triangular (non-conforming) | 4.27 | 0.08 $\sim$ 2.51 | Crouzeix and Raviart, 1973 |

**Table 2**. Summary of SSSC-OPF results with different small-signal constraints (Li et al., 2013 ).

| Cases | Generation cost ($/h) | Spectral abscissa | Cost increase | Iteration times | System stability status |
|---|---|---|---|---|---|
| base case | 3941.58 | -0.20 | 0.00% | 25 | Approaching critical stable |
| $\eta \leq$ -0.16 | 3941.58 | -0.20 | 0.00% | 46 | Approaching critical stable (no improvement) |
| $\eta \leq$ -0.25 | 3944.07 | -0.25 | 0.06% | 54 | Asymptotically stable (margin improved) |
| $\eta \leq$ -0.30 | 3947.93 | -0.30 | 0.16% | 49 | Asymptotically stable (margin increased) |
| $\eta \leq$ -0.35 | 3951.85 | -0.35 | 0.26% | 38 | Asymptotically stable (high margin) |
| $\eta \leq$ -0.40 | 3956.18 | -0.40 | 0.37% | 45 | Asymptotically stable (higher margin) |
| $\eta \leq$ -0.45 | 3960.27 | -0.45 | 0.47% | 58 | Asymptotically stable (optimal margin) |
| min($\eta$) | 4083.93 | -0.525 | 3.61% | 69 | Asymptotically stable (max margin) |

real parts. It is in a critically stable when some eigenvalues have zero real parts, and unstable when any eigenvalues have positive real parts. Based on this principle, researchers proposed a nonlinear semidefinite programming (NLSDP) model and algorithm for eigenvalue optimization (Li et al., 2013). Numerical results demonstrate that this method effectively solves the optimal power flow problem with small-signal stability constraints. The specific SSSC-OPF results under different spectral abscissa constraints are summarized in Table 2, and the generation costs for different $\eta$ values are shown in Fig. 1.

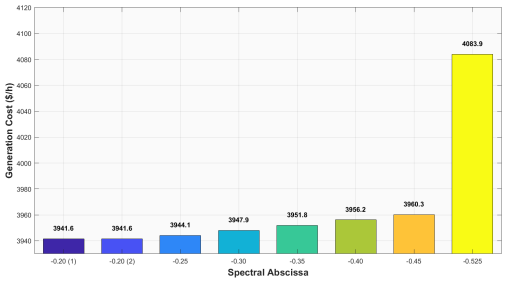


**Fig. 1**. Column chart of generation cost under spectral abscissa constraint.

According to small-signal stability theory, Table 2 showed that generation cost increased as small-signal stability constraints became more binding, and the transition of the system's stable state from near-critical stability to an optimal stability margin indicated that its anti-interference capability was gradually improving. Specifically, within the reasonable constraint interval of $-0.45 \leq \eta \leq -0.25$, only a 0.06% to 0.48% cost increase was required to achieve the substantial improvement from "approaching critical stability" to "asymptotic stability". This constitutes the optimal trade-off between economy and security, which fully satisfies the practical engineering requirements of power systems. At the same time, the reasonable increase in the number of iterations indicated that the algorithm exhibited excellent convergence and robustness. Thus, SSSC-OPF can strike a balance between the small-signal stability constraints and the higher generation cost. Additionally, in structural vibration control, the natural frequencies of a structure correspond to the eigenvalues of its stiffness matrix (Schwarzendahl et al., 2012; Coh et al., 2017), while in renewable energy grid integration systems, voltage stability can be evaluated via the minimum eigenvalue of the admittance matrix (Huang et al., 2017).

## 2.3 Application of eigenvalues in chemisorption

In chemical adsorption studies (Brenig and Schönhammer, 1974; Gomer, 1975), quantifiable descriptors can be identified and corresponding predictive models can be constructed by correlating the energy levels (i.e. eigenvalues) of electronic structures with adsorption strength, activation ability, and catalytic activity. A prominent representative is the Newns-Anderson model (Norsko et al., 1990), whose core idea is to simplify the interaction between the adsorbate and the metal surface as the coupling between the adsorbate orbitals and the metal bands, and to understand the adsorption process by solving the corresponding eigenvalue problem. As core mathematical tools for quantifying chemisorption, eigenvalues

**Table 3**. Eigenvalue descriptors corresponding to different carrier types and research objectives.

| Carrier type | Research objective | Eigenvalue descriptors | Reference |
|---|---|---|---|
| Metal | Adsorption strength | *d*-band center/DOS peak | Hammer and Norskov, 1995 |
| Metal | Catalytic activity | *d*-band center/DOS at Fermi level | Greeley and Mavrikakis, 2004 |
| Semiconductor | Adsorption selectivity | Band gap/VBM position | Chaves et al., 2020 |
| Semiconductor | Catalytic activity | CBM position/carrier concentration | Walter et al., 2010 |
| Insulator | Adsorption stability | Charge distribution at adsorption sites | Pacchioni, 2013 |

have been widely applied in various systems, including transition metal surfaces (Zheng et al., 2013), single-atom catalysts (Ren et al., 2022; Wang et al., 2025), alloy materials (Lü et al., 2013; Huang et al., 2018), and two-dimensional functional materials (Li et al., 2021; Li and Wang, 2024). For instance, the *d*-band center of transition metals (a weighted average of *d*-orbital eigenvalues) can directly predict the adsorption strength of small molecules and has become a core descriptor for catalyst design (Nørskov et al., 2004; Montemore and Medlin, 2014); changes in the bandgap eigenvalues of two-dimensional materials can intuitively reflect adsorption-induced electronic structure reconstruction, thereby laying a foundation for the development of gas sensors (Huzaifa et al., 2024; Patra et al., 2025). In chemical adsorption research, appropriate eigenvalue descriptors should be selected based on the carrier type and research objectives, with some related details summarized in Table 3.

Furthermore, chemisorption, as a crucial process in surface science and catalytic reactions, involves molecular interactions and is significant for investigating catalyst design, environmental pollution control, energy conversion, and other related fields. Density functional theory (DFT), a core theory in modern computational chemistry, is widely applied to the computation of electronic structures of substances. It holds significant scientific value and broad application prospects, particularly in areas such as chemical reactions, material design, catalytic processes, and energy engineering. In recent years, with the advancement in computing power and algorithm development, DFT has played a pivotal role in describing the electronic behavior of complex systems and predicting reaction mechanisms in chemisorption processes. However, DFT's computational complexity and convergence issues, particularly for large-scale systems, hinder its widespread application. Therefore, for the Kohn-Sham DFT model in chemisorption problems, it is of great significance and practical value to construct efficient structure-preserving numerical algorithms, which can enhance computational efficiency and convergence, resolve the computational challenges of current methods in large-scale complex systems, and advance DFT applications in chemistry, materials science, environmental science, and energy engineering–particularly practical applications in energy and environmental protection.

Molecular simulation (MD) technology was employed to investigate fluid behavior (including adsorption) in porous media as early as 2010. While classical force-field MD is relatively accurate for physisorption's study, quantum chemical calculations or MD simulations based on force fields derived from quantum mechanical calculations must be employed for chemisorption studies. Quantum chemical calculations for chemisorption (hereinafter referred to as quantum chemical calculations) are currently still lacking in energy research fields such as shale oil and gas development, underground $CO_2$ sequestration, and geological hydrogen storage. For the quantum chemical calculations of chemisorption, DFT is currently the most widely used dimensionality reduction algorithm. For the quantum chemical calculations of chemisorption, DFT is currently the most widely used dimensionality reduction algorithm (Nair et al., 2023, 2023a, 2024, 2024a, 2024b, 2025). During the research work of DFT, scientists gradually realized drawbacks and limitations of the algorithms integrated into commercial quantum chemistry software, one example as illustrated in Fig. 2. Consequently, the development of novel algorithms for DFT calculations has been attempted recently; for example, one unconditionally stable iterative algorithm has been proposed to replace DFT's SCF (self-consistent field) iterations (Wang et al., 2024).

## 2.4 The relationship between eigenvalues and quantum mechanics

In quantum mechanics research (Gasiorowicz, 2003; Griffiths and Schroeter, 2018), the core is to correlate the physically observable quantities of microscopic systems (e.g., energy, angular momentum) with operator eigenvalues. Specifically, the measured value of any physical quantity must be an eigenvalue of the corresponding self-adjoint operator, while the measurement probability is determined by the modulus squared of the expansion coefficient of the quantum state in the basis of the operator's eigenfunctions.

A typical representative is the single-particle steady-state Schrödinger equation (Schrödinger, 1926; Golebiewski and Taylor, 1967). The core idea of this equation is to transform the energy of the microsystem into the eigenvalue problem of the Hamiltonian operator. By solving for the operator's eigenvalues and eigenfunctions, we can not only determine the allowed quantum states of the system but also accurately predict the observed values of physical quantities. The expression $E_n = -13.6/n^2\text{eV}$ (where $n$ is the principal quantum number) is the eigenvalue of the Hamiltonian operator and corresponds to the allowed energy levels of the microscopic system. The discrete spectral lines observed in the experiment are shown in Fig. 3. Each horizontal line in the figure corresponds to the energy levels of different principal quantum numbers $n$, and

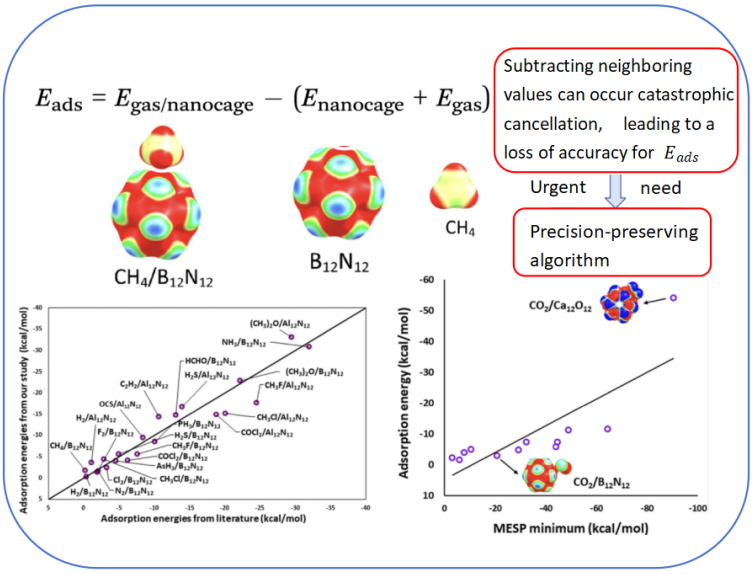


**Fig. 2**. The significance of accuracy-preserving algorithms in the chemical adsorption problem (Nair et al., 2023a; Nair et al., 2024b).

the marked energy values are in perfect agreement with the calculation results derived from the formula $E_n$ (Bohr, 1913; Eckert, 2013), which intuitively demonstrates the quantization characteristic of energy.

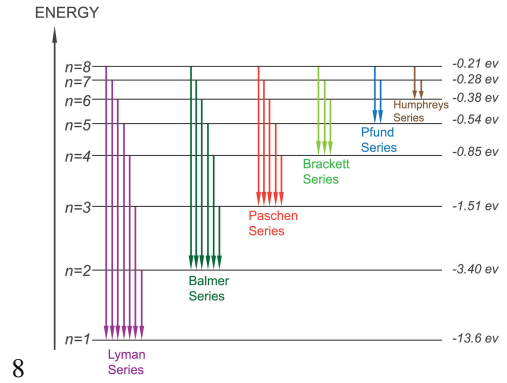


**Fig. 3**. The spectrum lines of hydrogen atoms.

Meanwhile, the arrows of different colors in the figure represent the electronic transitions between energy levels: purple arrows correspond to the Lyman series for $n \to 1$, and green arrows correspond to the Balmer series for $n \to 2$. The energy difference of each arrow (indicated by the arrow length) corresponds to the energy of the emitted photon, and the set of these transitions exactly matches the discrete spectral line series observed in the experiment. Thus, the figure clearly validates that "the hydrogen atom energy eigenvalue formula perfectly matches the experimentally observed spectral line series." This "operator-eigenvalue-physical quantity" correspondence forms the cornerstone of quantum mechanics theory (Dirac, 1981). Whether it is the eigenvalue $l(l+1)\hbar^2$ (where $l$ is the angular quantum number) of the orbital angular momentum operator $\hat{L}^2$ in angular momentum quantization (Jackiw, 2018), or the eigenvalue $\pm\frac{1}{2}\hbar$ of the electron spin operator, the discreteness of eigenvalues reveals the quantum nature of the microscopic world. This provides core theoretical support for atomic structure analysis, magnetic material design, quantum computing, and other related fields (Van Vleck, 1932; Nielsen and Chuang, 2010).

For multiparticle systems, the Schrödinger equation is employed to characterize a molecular systems consisting of $M$ atomic nuclei and $N_e$ electrons. It provides all the information about the system, including binding energy, electron affinity, molecular softness, absolute hardness, chemical potential, nucleus-independent chemical shift (NICS), and molecular electrostatic potential (MESP). However, directly solving this equation is extremely complex because it is an inseparable partial differential equation whose primary unknown is the wave function. It is a function of $3(N_e+M)$ independent variables representing spatial positions, and the complexity of the problem grows exponentially with the increase in the number of electrons and nuclei. To simplify the complexity of the problem, the Born-Oppenheimer (BO) approximation (Born and Oppenheimer, 1927) is introduced, which reduces the multi-particle Schrödinger equation to the time-independent Schrödinger equation for a multi-electron system (see Fig. 4).

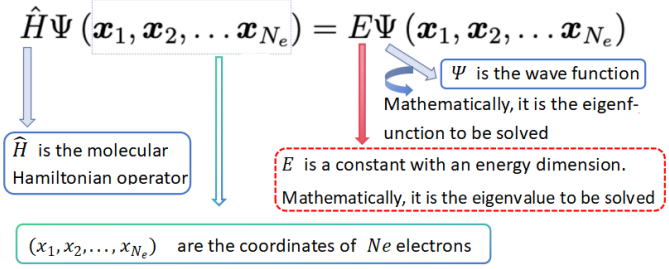


**Fig. 4**. Time-independent Schrödinger equation for a multi-electron system.

The BO approximation assumes that the mass of atomic

nuclei is much larger than that of electrons, therefore, nuclear motion can be neglected, and the electrons are treated as moving within a fixed nuclear framework. Through this approximation, we can decouple the many-body problem into independent electronic and nuclear components, thereby significantly reducing the computational complexity. The BO approximation assumes that atomic nuclei are far more massive than electrons. Therefore, nuclear motion can be neglected, allowing the electrons to be treated as moving within a fixed nuclear framework. Through this approximation, we can decompose the multi-body problem into two independent subproblems corresponding to the electronic part and the nuclear part respectively, thereby significantly reducing the computational complexity. Nevertheless, even after the system is simplified to an electronic problem via the BO approximation, it remains a high-dimensional linear eigenvalue problem. Specifically, assuming there are $N_e$ electrons in the system and each electron has three spatial coordinates, the electronic wave function is a function of $3N_e$ independent variables. As the number of electrons increases, the dimensionality of the system rises rapidly, which leads to an exponential growth in computational load and storage requirements.

This high-dimensional growth leads to the well-known curse of dimensionality, making the problem essentially intractable. As the number of electrons increases, the storing, processing, and solving for the wave function become extremely challenging. Currently, various computational methods have been developed to address multi-electron systems, including wave function-based methods, Density Functional Theory (DFT), and quantum Monte Carlo methods. Among these approaches, wave function methods and DFT are most representative. The wave function method is one of the mainstream approaches in the field of quantum chemistry (Sherrill and Schaefer, 1999), it calculates the electronic wave function of a system by solving the multi-body Schrödinger equation, thereby deriving the system's energy and other physical properties. Although the wave function method has high accuracy, its computational cost is prohibitive. Especially when dealing with multi-electron systems, the computational complexity is substantial, which limits its application to large-scale systems.

To reduce the computational complexity, DFT is introduced. It describes a multi-electron systems via electron density rather than wave functions, transforming the multi-body wave function problem into a single-particle problem. Herein, the electronic density only depends on spatial coordinates, reducing the originally high-dimensional multi-electron problem to a three-dimensional one and significantly lowering the computational complexity, as illustrated in Fig. 5. The idea of DFT can be traced back to the Thomas-Fermi model proposed by Thomas and Fermi in 1927. In 1964, Hohenberg and Kohn (1964) proposed the Hohenberg-Kohn theorem, which states that a system's ground-state energy is a unique functional of the electron density and that the external potential can be determined by the electron density. Subsequently, Kohn and Sham (1965) further developed this theory and proposed the Kohn-Sham equations. Specifically, by constructing an uninteracting system, the complex multi-electron Schrödinger equation is transformed into a simple single-electron problem. Then, an exchange-correlation functional is modeled to correct the deviations caused by the approximation of the non-interacting system.

The earliest solution method for Kohn-Sham DFT is the direct energy minimization method (Francisco et al., 2004; Jiang and Dai, 2015). However, due to orthogonality constraints, maintaining the orthogonality of orbitals becomes a major challenge for this method. This usually requires additional algorithmic strategies and involves enormous computational complexity. Based on the variational principle and the differentiability of the energy functional, the energy minimization problem can be transformed into the following nonlinear eigenvalue problem on a three-dimensional space:

$$\left(-\frac{1}{2}\Delta + V_{\text{eff}}(\rho_\Psi)\right)\psi_i(\mathbf{r}) = \varepsilon_i\psi_i(\mathbf{r}), \quad \text{in } \mathbb{R}^3$$

$$\int_{\mathbb{R}^3} \psi_i(\mathbf{r})\psi_j(\mathbf{r})\,d\mathbf{r} = \delta_{ij}, \ i,j = 1,2,\ldots,N$$

The self-consistent field (SCF) iteration method is a traditional approach for solving nonlinear eigenvalue problems. It solves the Kohn-Sham equations by repeatedly applying fixed-point iteration until the self-consistency condition is satisfied. While this method is effective for small-scale systems, its convergence is unsatisfactory for small-band-gap systems. Especially in the calculation of large-scale systems, the convergence behavior of SCF iteration becomes unpredictable, resulting in low computational efficiency (Liu et al., 2014, 2015; Dai et al., 2017). The earliest numerical analysis of nonlinear eigenvalue problems was proposed by Zhou (2003), which established the convergence of the finite-dimensional approximation of the Gross-Pitaevskii equation for Bose-Einstein condensates. Chen et al. (2013) conducted a systematic a priori error analysis of arbitrary finite-dimensional discretizations of the Kohn-Sham equations under the assumption of local diffeomorphism, and proved that the limit of any finite-dimensional discretization converges to the ground state under appropriate conditions. Subsequently, Chen et al. (2014) further performed a posteriori error analysis of the finite element discretization of the Kohn-Sham equations.

The gradient flow method, as a novel strategy for solving the Kohn-Sham equations, has attracted considerable attention (Bao and Du, 2004; Yang and Ju, 2017; Shen et al., 2019). In the gradient flow model, the concept of gradient flow is introduced, and the Kohn-Sham energy functional is regarded as a dynamic process, thereby finding the lowest energy state of the system through a flow-based approach. Unlike the SCF iteration method and the direct energy minimization method, the gradient flow method has unique advantages in structure preservation. It can maintain orbital orthogonality without explicit orthogonalization operations, avoiding the computational overhead of traditional methods. Dai et al. (2020) proposed a model that can simultaneously ensure energy stability and satisfy orthonormality constraints of orbitals by introducing an extended gradient within a continuous framework. This property provides a foundation for designing numerical discretization methods that are unconditionally energy-stable and orthonormality-preserving. Fig. 6 outlines the solution strategy for Kohn-Sham DFT.

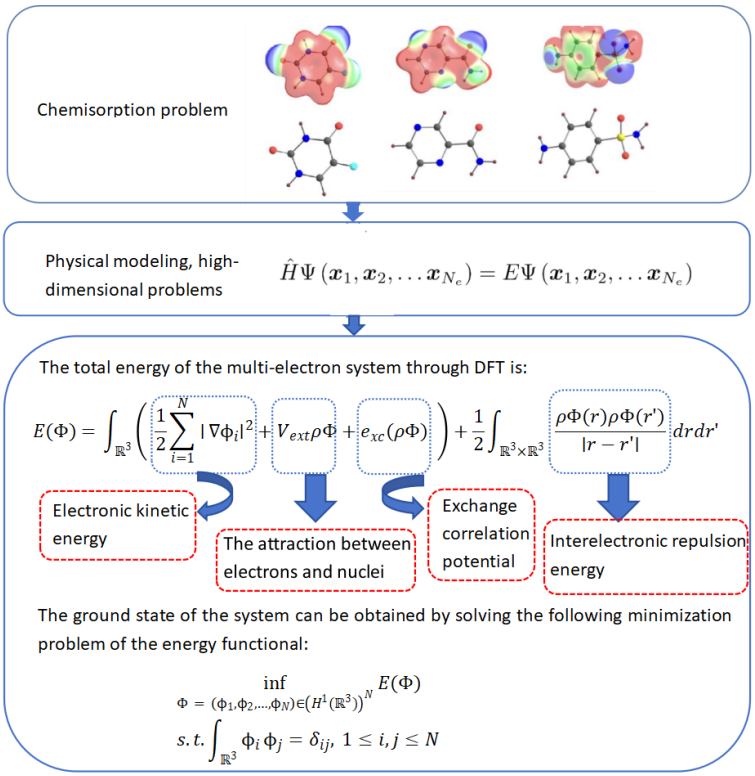


**Fig. 5**. The dimensionality reduction model of density functional theory.

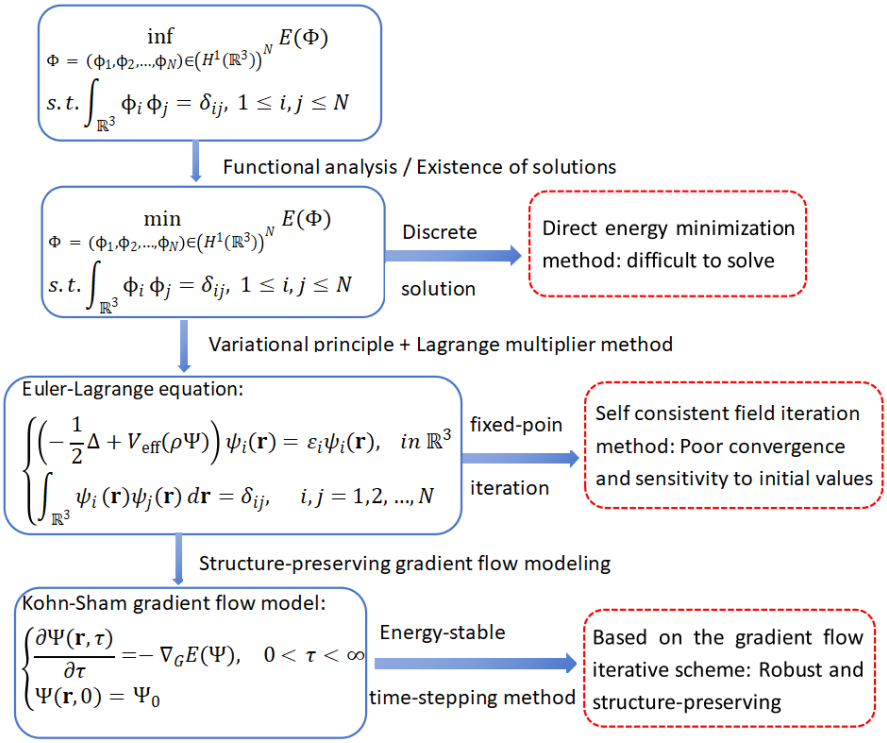


**Fig. 6**. Different solving strategies of density functional theory.

In recent years, unconditionally energy-stable numerical discretization methods, represented by the numerical solution of gradient flows, have gained recognition in the academia, particularly for problems involving multi-component, multi-phase flows, and transport phenomena (Feng et al., 2022; Shen et al., 2022). Since these problems typically involve strong nonlinearity, multi-physics coupling, and non-convexity of the background energy, traditional methods often require the use of small time steps to ensure computational stability. However, when only conditional energy stability is satisfied, the use of small time steps may severely reduce computational efficiency. Therefore, constructing unconditionally energy-stable discretization schemes is crucial, it cannot only improve the computational efficiency of numerical simulations but also enhance the robustness of calculations, thereby playing a key role in the numerical solution of complex systems.

## 3. Robust algorithms for solving the smallest eigenvalue

Next, we will introduce in detail a robust algorithm for solving the smallest eigenvalue, which can be extended to computing the first $m$ smallest eigenvalues. This section focuses on the robust algorithm for solving the smallest eigenvalue.

### 3.1 Gradient flow based model

The smallest eigenvalue $\lambda_{\min}$ of a symmetric matrix $A \in \mathbb{R}^{n\times n}$ is given by the solution of the following constrained minimization problem:

$$\lambda_{\min} = \min_{v\in\mathbb{R}^n} \frac{1}{2}(Av, v) \quad \text{subject to} \quad \|v\|_2 = 1$$

where $E(v) = \frac{1}{2}(Av, v)$, the constraint defines the unit sphere $S^{n-1} \subset \mathbb{R}^n$, which is a compact set that ensures the existence of a minimum.

Introducing the Stiefel manifold:

$$\mathscr{M} = \left\{v \in \mathbb{R}^n \mid v^T v = I\right\}$$

Then the gradient of $\nabla E(v)$ on the Stiefel manifold is:

$$\nabla_G E(v) = \nabla E(v) - v(v^T \nabla E(v))$$

where $v(v^T \nabla E(v))$ is the component of $\nabla E(v)$ along the direction of $v$, and this component is subtracted to ensure orthogonality.

To facilitate the design of length-preserving numerical solutions, we extend the gradient flow $\nabla_G E(v)$ from the manifold $\mathscr{M}$ to the entire space $\mathbb{R}^n$. We denote the extended gradient flow by $\nabla_{\mathbb{G}} E(v)$, which is defined as:

$$\nabla_{\mathbb{G}} E(v) = (v, v)\nabla E(v) - v(v^T \nabla E(v))$$

Different from the eigenvalue energy minimization model, we consider the following gradient flow model:

$$\begin{cases} \dfrac{dv}{dt} = -\nabla_{\mathbb{G}} E(v), \ 0 < t < \infty \\ v(t=0) = u_0, \quad \|v_0\|_2 = 1 \end{cases} \tag{1}$$

where $\nabla_{\mathbb{G}} E(v) = (v, v)Av - (Av, v)v$, $A$ is a symmetric positive-definite matrix.

**Theorem 3.1.** *When $\|v(0)\| = 1$ and $A$ is a symmetric positive definite matrix, the gradient flow in Eq. (1) possesses the properties of length preservation and energy dissipation, and it holds that:*

$$\|v\| = 1, \quad \frac{dE}{dt} \le 0$$

*Proof.* From Eq. (1), we have:

$$\begin{aligned} \frac{d}{dt}\|v\|^2 = 2\left(v, \frac{dv}{dt}\right) &= -2\left(v, (v, v)Av - (Av, v)v\right) \\ &= -2\|v\|^2(v, Av) + 2(Av, v)\|v\|^2 = 0 \end{aligned}$$

Thus, when the initial condition $\|v(0)\| = 1$ is satisfied, $\|v(t)\| = 1$ holds for all $t \ge 0$. This proves that the solution to the gradient flow Eq. (1) remains on the manifold at all times. Let $E(v) = \frac{1}{2}(Av, v)$, by the Cauchy-Schwarz inequality, we have $(Av, v)^2 \le \|Av\|^2\|v\|^2$, thus:

$$\begin{aligned} \frac{dE}{dt} = \left(Av, \frac{dv}{dt}\right) &= \left(Av, -(v, v)Av + (Av, v)v\right) \\ &= \left[-\|v\|^2\|Av\|^2 + (Av, v)^2\right] \le 0 \end{aligned}$$

Hence:

$$\frac{dE}{dt} \le 0$$

This implies that the Eq. (1) satisfies the property of energy dissipation for all $t \ge 0$. □

**Theorem 3.2.** *When the initial condition $\|v_0\| = 1$ is satisfied, the gradient flow Eq. (1) has the global existence and uniqueness of solutions.*

*Proof.* Let $f(v) = -[(v, v)Av - (Av, v)v]$, clearly $f \in C^\infty$. By Theorem 3.1, for any $v_1, v_2$, we have $\|v_0\| = \|v_1\| = \|v_2\| = 1$, thus:

$$\begin{aligned} f(v_1) - f(v_2) = &-A(v_1 - v_2) + (Av_1, v_1)(v_1 - v_2) \\ &+ \left[(A(v_1 - v_2), v_1) + (Av_2, v_1 - v_2)\right]v_2 \end{aligned}$$

Taking the norm of both sides and applying the triangle inequality, we obtain:

$$\begin{aligned} \|f(v_1) - f(v_2)\| \le &\|-A(v_1 - v_2)\| + \|(Av_1, v_1)(v_1 - v_2)\| \\ &+ \|(A(v_1 - v_2), v_1)v_2\| + \|(Av_2, v_1 - v_2)v_2\| \end{aligned}$$

Applying the Cauchy-Schwarz inequality and the property of operator norm, we have:

$$\|f(v_1) - f(v_2)\| \le 4\|A\|\|v_1 - v_2\|$$

That is, $f$ satisfies the Lipschitz condition with constant $L = 4\|A\|$.

By the Picard-Lindelöf existence and uniqueness theorem, a local solution exists and is unique. According to Theorem 3.1 and the extension theorem for solutions of ordinary differential equations, this local solution can be extended indefinitely on the sphere, thus yielding the existence of a global solution. We now proceed to prove the uniqueness of the global solution.

For Eq. (1), suppose there exist two solutions $v_1(t)$ and $v_2(t)$. Define the difference as $w(t) = v_1(t) - v_2(t)$, then $w(0) = 0$. Thus:

$$\begin{aligned}\frac{dw}{dt} &= -Aw + [(Av_1, v_1)v_1 - (Av_2, v_2)v_2] \\ &= -Aw + (Aw, v_1)v_1 + (Av_2, w)v_1 + (Av_2, v_2)w\end{aligned}$$

and

$$\frac{d}{dt}\|w\|^2 = 2\left(w, \frac{dw}{dt}\right) = -2(w, Aw) + 2\left[(Aw, v_1)(w, v_1) + (Av_2, w)(w, v_1) + (Av_2, v_2)\|w\|^2\right]$$

Due to the symmetric positive definiteness of $A$, we have $(w, Aw) \geq \lambda_{\min}(A)\|w\|^2$, where $\lambda_{\min}(A)$ denotes the smallest eigenvalue of $A$. Then, utilizing the Cauchy-Schwarz inequality and properties of the operator norm, we arrive at the following result:

$$\frac{d}{dt}\|w\|^2 \leq -2\lambda_{\min}(A)\|w\|^2 + 6\|A\|\|w\|^2 = L\|w\|^2$$

where $L = 6\|A\| - 2\lambda_{\min}(A)$. Let $u(t) = \|w(t)\|^2$, then $u(0) = 0$, we have:

$$\frac{du}{dt} \leq Lu(t), \quad t \geq 0$$

By the Grönwall inequality:

$$u(t) \leq u(0)e^{\int_0^t L ds} = u(0)e^{Lt} = 0$$

Since $u(t) = \|w(t)\|^2 \geq 0$, it follows that $u(t) = 0$, i.e., $v_1(t) \equiv v_2(t)$. Hence, the solution is unique. In conclusion, the gradient flow Eq. (1) admits a unique global solution. □

## 3.2 Discrete scheme

In this section, we present a length-preserving and unconditionally energy-stable discrete scheme for computing the smallest eigenvalue. The details are as follows:

$$\frac{v^{k+1} - v^k}{\Delta t} = -\left[(v^{k+\frac{1}{2}}, v^{k+\frac{1}{2}})Av^{k+\frac{1}{2}} - (Av^{k+\frac{1}{2}}, v^{k+\frac{1}{2}})v^{k+\frac{1}{2}}\right] \tag{2}$$

where $v^{k+\frac{1}{2}} = \frac{1}{2}(v^{k+1} + v^k)$.

**Theorem 3.3.** *The numerical solution of the scheme Eq. (2) satisfies:*

$$\|v^{k+1}\| = \|v^k\| = 1, \quad E(v^{k+1}) \leq E(v^k)$$

*Proof.* Taking the inner product of $v^{k+\frac{1}{2}}$ with both sides of the discrete scheme Eq. (2), we have:

$$\frac{\|v^{k+1}\|^2 - \|v^k\|^2}{2\Delta t} = 0$$

Thus, $\|v^{k+1}\|^2 - \|v^k\|^2 = 0$. Given the initial condition $\|v^0\| = 1$, it follows that $\|v^{k+1}\| = \|v^k\| = 1$ for all $k \geq 0$.

Define the energy function as $E(v^k) = \frac{1}{2}(Av^k, v^k)$. Taking the inner product of $Av^{k+\frac{1}{2}}$ with both sides of the discrete scheme Eq. (2), we obtain:

$$\frac{E(v^{k+1}) - E(v^k)}{\Delta t} = -\|v^{k+\frac{1}{2}}\|^2\|Av^{k+\frac{1}{2}}\|^2 + \left(v^{k+\frac{1}{2}}, Av^{k+\frac{1}{2}}\right)^2 \tag{3}$$

From the Cauchy-Schwarz inequality, it follows that:

$$\left(v^{k+\frac{1}{2}}, Av^{k+\frac{1}{2}}\right)^2 \leq \left\|v^{k+\frac{1}{2}}\right\|^2 \left\|Av^{k+\frac{1}{2}}\right\|^2$$

Substituting the above inequality into Eq. (3), we can derive that:

$$E(v^{k+1}) \leq E(v^k)$$

This completes our proof. □

## 3.3 Numerical experiments

In this section, we derive a fully discrete scheme by applying the finite difference method under homogeneous Dirichlet boundary conditions, as follows:

$$\frac{v_h^{k+1} - v_h^k}{\Delta t} = -\left[(v_h^{k+\frac{1}{2}}, v_h^{k+\frac{1}{2}})Av_h^{k+\frac{1}{2}} - (Av_h^{k+\frac{1}{2}}, v_h^{k+\frac{1}{2}})v_h^{k+\frac{1}{2}}\right]$$

where $v_h^{k+\frac{1}{2}} = \frac{1}{2}(v_h^{k+1} + v_h^k)$. Obviously, this fully discrete scheme also possesses the properties of length preservation and energy dissipation, due to Theorem 3.3.

Next, to validate the effectiveness of our algorithm, we consider the eigenvalue problem: $-\Delta u = \lambda u$ on the domain $\Omega = [0, 1] \times [0, 1]$ with homogeneous Dirichlet boundary conditions, $u(0)$ is an arbitrary eigenvector satisfying $\|u(0)\| = 1$. Let $\lambda_{\text{theory}}$ and $\lambda_h$ denote the smallest theoretical eigenvalue and numerical eigenvalue, respectively. The error between them is defined as:

$$e(\lambda_{theory}, \lambda_h) = \|\lambda_{theory} - \lambda_h\|_{L^\infty(\Omega)}$$

Table 4 lists the errors between the smallest theoretical eigenvalues and the corresponding numerical eigenvalues for different grid sizes at $\Delta t = 1$. Fig. 7 shows the evolution of the total energy with respect to the number of iterations for the mesh with $h = \frac{1}{320}$. From Table 4, it can be observed that our method remains efficient even with large time steps. Fig. 7 demonstrates the dissipation of total energy as the number of iterations increases. This further indicates that our method is unconditionally energy-stable even with large time steps.

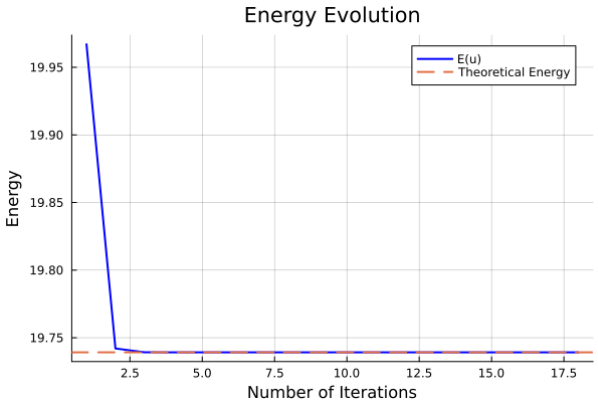


**Fig. 7**. The evolution of the total energy for $h = \frac{1}{320}$.

**Table 4**. The error results of the smallest eigenvalue with $\Delta t = 1$.

| $h$ | $\lambda_{theory}$ | $\lambda_h$ | $e(\lambda, \lambda_h)$ |
|---|---|---|---|
| 1/10 | 19.739208802179 | 19.675574494181 | 6.363431e-02 |
| 1/20 | 19.739208802179 | 19.737586098044 | 1.622704e-03 |
| 1/40 | 19.739208802179 | 19.739161696735 | 4.710544e-05 |
| 1/80 | 19.739208802179 | 19.739207203862 | 1.598317e-06 |
| 1/160 | 19.739208802179 | 19.739208739976 | 6.220284e-08 |
| 1/320 | 19.739208802179 | 19.739208799382 | 2.797059e-09 |

## 4. Robust algorithm for solving the first $m$ smallest eigenvalues

In this section, we present a length-preserving and unconditionally energy-stable algorithm for computing the first $m$ smallest eigenvalues of the gradient flow, and we prove the existence and uniqueness of solutions for the proposed algorithm. The specific details of this algorithm are as follows.

First, we solve for the smallest eigenpair $(\lambda_1, u_1)$ via the scheme formulation below:

$$\frac{\partial v}{\partial t} = -\left[(v,v)Av - (Av,v)v\right]$$

where $\|v(0)\| = 1$. Then, by imposing the constraint $v(0) \perp u_1$, the second smallest eigenpair $(\lambda_2, u_2)$ can be derived from the subsequent equation:

$$\frac{\partial v}{\partial t} = -\left[(v,v)Av - (Av,v)v - (Av,u_1)u_1\right]$$

By analogy, when the first ($m$-1) smallest eigenvalues of $A$ are known, a recursive algorithm for computing the $m$-th smallest eigenvalue can be obtained, with its specific form given as:

$$\begin{cases} \dfrac{\partial v}{\partial t} = -\left[(v,v)Av - (Av,v)v - \displaystyle\sum_{i=1}^{m-1}(Av,u_i)u_i\right] \\ \|v(0)\| = 1, v(0) \perp u_i, i = 1, \cdots, m-1 \end{cases} \tag{4}$$

where $\{u_i\}$ are the eigenvectors of the symmetric positive definite matrix $A$, satisfying $Au_i = \lambda_i u_i$ and $u_i^T u_j = \delta_{ij}$.

**Theorem 4.1.** *For the algorithm Eq. (4), when the initial condition satisfies $\|v(0)\| = 1$, $v(0) \perp u_i$, we have:*

$$v(t) \perp u_i, \quad \|v(t)\| = 1, \quad \frac{dE}{dt} \le 0$$

*Proof.* Since $u_i$ is constant vector, we have:

$$\frac{\partial}{\partial t}(v,u_i) = \left(\frac{\partial v}{\partial t}, u_i\right)$$

Let $\alpha(t) = (v(t), u_i)$. From $Au_i = \lambda_i u_i$, $(u_i, u_j) = \delta_{ij}$, and the symmetric positive definiteness of $A$, we obtain $(Av, u_i) = (v, Au_i) = \lambda_i(v,u_i) = \lambda_i\alpha$ and $\sum_{j=1}^{m}(Av,u_j)(u_j,u_i) = \lambda_i\alpha$. Thus:

$$\frac{\partial \alpha}{\partial t} = -\left[\lambda_i\|v\|^2 - (Av,v) - \lambda_i\right]\alpha(t) = G(t)\alpha(t)$$

where $G(t) = -\left[\lambda_i\|v\|^2 - (Av,v) - \lambda_i\right]$. Obviously, this is a first-order linear ordinary differential equation for $\alpha(t)$, Given that the initial condition satisfies $v(0) \perp u_i$, i.e., $\alpha(0) = (v(0), u_i) = 0$, its solution satisfies:

$$\alpha(t) = \alpha(0)\exp\left(\int_0^t G(s)\,ds\right) = 0 \quad \Rightarrow \quad v(t) \perp u_i$$

Furthermore, we have:

$$\begin{aligned} &\frac{\partial}{\partial t}\|v\|^2 = 2\left(v, \frac{\partial v}{\partial t}\right) \\ &= 2\left[-\|v\|^2(v,Av) + (Av,v)\|v\|^2 + \sum_{i=1}^{m}(Av,u_i)(v,u_i)\right] = 0 \end{aligned}$$

So, when the initial condition is $\|v(0)\| = 1$, then $\|v(t)\| = 1$ for all $t \ge 0$.

Define the energy functional $E(v) = \frac{1}{2}(v,Av)$. Using $\|v\| = 1$, $(Av, u_i) = \lambda_i(v,u_i) = 0$ and Cauchy-Schwarz inequality, we derive that:

$$\begin{aligned} \frac{dE}{dt} = \left(Av, \frac{\partial v}{\partial t}\right) &= \left[-\|Av\|^2 + (Av,v)^2\right] \\ &\le \left[-\|Av\|^2 + \|Av\|^2\|v\|^2\right] = 0 \end{aligned}$$

Therefore $\frac{dE}{dt} \le 0$, which indicates that the energy decreases monotonically over time. □

### 4.1 Discrete scheme

The discrete counterpart of Eq. (4) takes the form of:

$$\begin{aligned} \frac{v^{k+1} - v^k}{\Delta t} = -\Big[&\|v^{k+\frac{1}{2}}\|^2 Av^{k+\frac{1}{2}} - (Av^{k+\frac{1}{2}}, v^{k+\frac{1}{2}})v^{k+\frac{1}{2}} \\ &- \sum_{i=1}^{m-1}(Av^{k+\frac{1}{2}}, u_i)u_i\Big] \end{aligned} \tag{5}$$

**Theorem 4.2.** *The numerical solution of the scheme Eq. (5) satisfies:*

$$v^{k+1} \perp u_i, \quad \|v^{k+1}\| = \|v^k\| = 1, \quad E(v^{k+1}) \le E(v^k)$$

*Proof.* Let $a = v^{k+\frac{1}{2}} = \frac{1}{2}(v^{k+1} + v^k)$. Taking the inner product of both sides of the discrete scheme in Eq. (5), we obtain:

$$\|v^{k+1}\|^2 - \|v^k\|^2 = 2\Delta t\sum_{i=1}^{m}(Aa,u_i)(u_i,a) \tag{6}$$

When $k = 0$, $(v^0, u_i) = 0$. Suppose for a certain $k$, $(v^k, u_i) = 0$ holds for all $i = 1, \ldots, m$. We next prove $v^{k+1} \perp u_i$ for all

$i = 1, \ldots, m$. Since $(u_j, u_i) = \delta_{ij}$, taking the inner product of the discrete scheme Eq. (5) with $u_j$ gives:

$$(v^{k+1} - v^k, u_j) = -\Delta t \left[(Aa, u_j)(\|a\|^2 - 1) - (Aa, a)(a, u_j)\right]$$

Using the symmetry of $A$ and the eigenvalue-eigenvector property ($Au_j = \lambda_j u_j$), we have $(Aa, u_j) = (a, Au_j) = \lambda_j (a, u_j)$. Utilizing $(v^k, u_i) = 0$ and $a = \frac{1}{2}(v^{k+1} + v^k)$, The above equation can be rewritten as:

$$2(a, u_j) = -\Delta t \cdot (a, u_j) \left[(\|a\|^2 - 1)\lambda_j - (Aa, a)\right]$$

If $(a, u_j) \neq 0$, we divide both sides by $(a, u_j)$ to obtain:

$$(\|a\|^2 - 1)\lambda_j - (Aa, a) = -\frac{2}{\Delta t}$$

The right-hand side is a constant (independent of $j$), whereas the left-hand side depends on $\lambda_j$ (which may vary with $j$). This leads to a contradiction, since the equation cannot hold for all $j$ in general. Therefore, $(a, u_j) = 0$ must hold for all $j = 1, \ldots, m$.

By using $(v^k, u_i) = 0$ and $a = \frac{1}{2}(v^{k+1} + v^k)$, we obtain:

$$(a, u_i) = \frac{1}{2}(v^{k+1}, u_i) = 0 \quad \Rightarrow \quad (v^{k+1}, u_i) = 0$$

Thus, $v^{k+1} \perp u_i$ for all $k$ and $i = 1, \ldots, m$.

Substituting $(a, u_i) = 0$ into Eq. (6) gives $\|v^{k+1}\|^2 - \|v^k\|^2 = 0$. Since $\|v^0\| = 1$, it follows that $\|v^{k+1}\| = \|v^k\| = 1$ for all $k \geq 0$.

From the orthogonality condition, we have $(v^{k+\frac{1}{2}}, u_i) = 0$ and $(u_i, Av^{k+\frac{1}{2}}) = (Au_i, v^{k+\frac{1}{2}}) = \lambda_i (u_i, v^{k+\frac{1}{2}}) = 0$. Obviously the discrete scheme Eq. (5) is equivalent to Eq. (2). Therefore, this discrete scheme possesses the properties of length preservation and energy dissipation. □

### 4.2 Numerical experiments

Similar to the previous numerical case, based on the discrete schemes Eq. (5), we obtain the errors of the first five smallest eigenvalues under different grid sizes at a time step of $\Delta t = 1$, as summarized in Table 5. Fig. 8 presents the energy dissipation curves corresponding to the first two smallest eigenvalues. The results in Table 5 and Fig. 8 demonstrate the effectiveness and energy stability, respectively, of our algorithm.

## 5. Conclusions

In this paper, we first briefly introduce the relationship between eigenvalue problems and various fields, as well as their applications in these fields. For instance, in energy engineering, eigenvalues can intuitively quantify system's stability, thereby guiding the control of electricity costs in power systems. We then elaborate on the difficulties encountered in solving eigenvalue problems in complex systems, emphasizing the importance of developing a robust gradient-flow-based algorithm to address these challenges. Finally, we present an efficient algorithm for solving the first $m$ smallest eigenvalues. This algorithm is capable of converging from arbitrary initial guesses to the first $m$ smallest eigenpairs, and its strict length preservation and unconditional energy stability endow it with high robustness throughout the entire computational process. Numerical experiments further demonstrate that it maintains stable convergence even with large time steps. In addition, the algorithm can be extended to both linear and nonlinear problems.

## Acknowledgements

We would like to express our appreciation to the support from National Key Research and Development Project of China (Grant No. 2023YFA1011701) and National Natural Science Foundation of China (Grant No. 12571466).

## Conflict of interest

The authors declare no competing interest.



## References

Auchmuty, G. Unconstrained variational principles for eigenvalues of real symmetric matrices. SIAM journal on mathematical analysis, 1989, 20(5): 1186-1207.

Auchmuty, G., Rivas, M. A. Unconstrained variational principles for linear elliptic eigenproblems. ESAIM: Control, Optimisation and Calculus of Variations, 2015, 21(1): 165-189.

Achtziger, W., Kočvara, M. Structural topology optimization with eigenvalues. SIAM Journal on Optimization, 2008, 18(4): 1129-1164.

Allen, E. J., Berry, R. M. The inverse power method for calculation of multiplication factors. Annals of Nuclear Energy, 2002, 29(8): 929-935.

Betcke, T., Voss, H. A Jacobi-Davidson-type projection method for nonlinear eigenvalue problems. Future Generation Computer Systems, 2004, 20(3): 363-372.

Botchev, M. A., Sleijpen, G. L. G., Sopaheluwakan, A. An SVD-approach to Jacobi-Davidson solution of nonlinear Helmholtz eigenvalue problems. Linear algebra and its applications, 2009, 431(3-4): 427-440.

Brenner, S. C., Scott, L. R. The mathematical theory of finite element methods. New York, NY, USA, Springer, 2008.

Braess, D. Finite elements: Theory, fast solvers, and applications in solid mechanics (3rd ed). Cambridge, England, Cambridge University Press, 2007.

Banjai, L., Boulton, L. Computation of sharp estimates of the Poincaré constant on planar domains with piecewise self-similar boundary. Journal of Fractal Geometry, 2021, 8(2): 153-188.

Bohr, N. On the constitution of atoms and molecules. The London, Edinburgh, and Dublin Philosophical Magazine and Journal of Science, 1913, 26(153): 476-502.

Brenig, W., Schönhammer, K. On the theory of chemisorption. Zeitschrift für Physik, 1974, 267(3): 201-208.

Budd, C. J., Piggott, M. D. Geometric integration and its applications. Handbook of Numerical Analysis, 2003, 11: 35-139.

**Table 5**. The error results of the first five smallest eigenvalues with $\Delta t = 1$.

| $h$ | $\lambda_1$ | $\lambda_2$ | $\lambda_3$ | $\lambda_4$ | $\lambda_5$ |
|---|---|---|---|---|---|
| 1/10 | 6.363431e-02 | 1.103041e+00 | 1.103042e+00 | 1.993367e+00 | 5.873835e+00 |
| 1/20 | 1.622704e-03 | 4.595904e-02 | 4.595908e-02 | 8.453974e-02 | 4.535623e-01 |
| 1/40 | 4.710541e-05 | 1.469082e-03 | 1.469088e-03 | 2.498354e-03 | 1.727449e-02 |
| 1/80 | 1.598203e-06 | 4.962507e-05 | 4.962527e-05 | 7.708592e-05 | 6.449094e-04 |
| 1/160 | 6.216792e-08 | 1.940589e-06 | 1.939385e-06 | 2.294894e-06 | 2.688140e-05 |
| 1/320 | 2.735423e-09 | 7.935080e-08 | 7.744305e-08 | 8.180531e-08 | 1.284746e-06 |

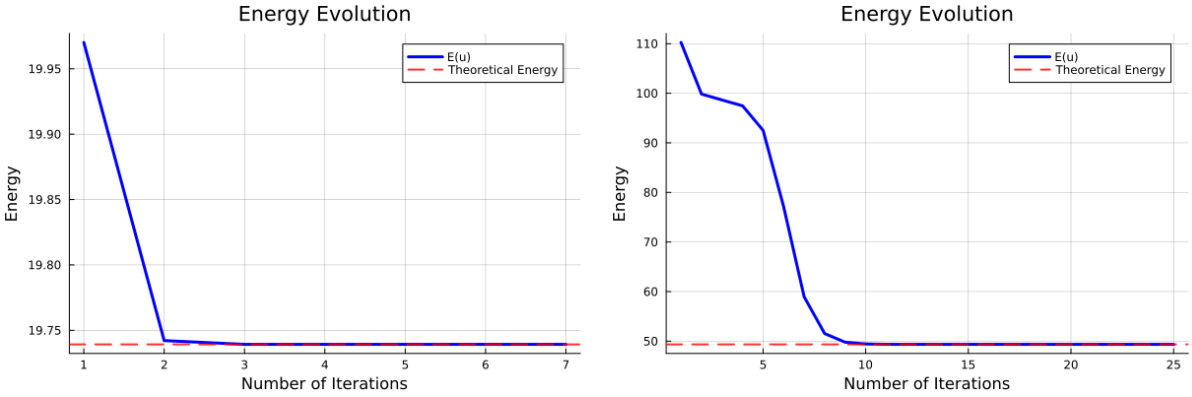


(a) (b)

**Fig. 8**. The total energy evolution figure of the first two smallest eigenvalues $\lambda_1$ (left) and $\lambda_2$ (right) when $h = \frac{1}{320}$.


Born, M., Oppenheimer, R. Zur quantentheorie der molekeln. Annalen der Physik, 1927, 389(20): 457-484.

Bao, W., Du, Q. Computing the ground state solution of Bose-Einstein condensates by a normalized gradient flow. SIAM Journal on Scientific Computing, 2004, 25(5): 1674-1697.

Ciarlet, P. G. The finite element method for elliptic problems. Amsterdam, Netherlands, North-Holland Publishing Company, 1978.

Crouzeix, M., Raviart, P. A. Conforming and nonconforming finite element methods for solving the stationary Stokes equations I. Revue française d'automatique informatique recherche opérationnelle. Mathématique, 1973, 7(R3): 33-75.

Ciarlet, P. G. The finite element method for elliptic problems. Philadelphia, USA, Society for Industrial and Applied Mathematics, 2002.

Chaves, A., Azadani, J. G., Alsalman, H., et al. Bandgap engineering of two-dimensional semiconductor materials. npj 2D Materials and Applications, 2020, 4(1): 29.

Canfield, R. A. Design of frames against buckling using a Rayleigh quotient approximation. American Institute of Aeronautics and Astronautics Journal, 1993, 31(6): 1143-1149.

Coh, S., Yu, P. Y., Aoki, Y., et al. Alternative structure of $TiO_2$ with higher energy valence band edge. Physical Review B, 2017, 95(8): 085422.

Chen, H., Gong, X., He, L., et al. Numerical analysis of finite dimensional approximations of Kohn-Sham models. Advances in Computational Mathematics, 2013, 38(2): 225-256.

Chen, H., Dai, X., Gong, X., et al. Adaptive finite element approximations for Kohn-Sham models. Multiscale Modeling & Simulation, 2014, 12(4): 1828-1869.

Dai, X., Liu, Z., Zhang, L., et al. A conjugate gradient method for electronic structure calculations. SIAM Journal on Scientific Computing, 2017, 39(6): A2702-A2740.

Dai, X., Wang, Q., Zhou, A. Gradient flow based Kohn-Sham density functional theory model. Multiscale Modeling & Simulation, 2020, 18(4): 1621-1663.

Dirac, P. A. M. The principles of quantum mechanics. Oxford, UK, Oxford University Press, 1981.

Durán, R. G., Gastaldi, L., Padra, C. A posteriori error estimators for mixed approximations of eigenvalue problems. Mathematical Models and Methods in Applied Sciences, 1999, 9(8): 1165-1178.

Eckert, M. Sommerfeld's atombau und spektrallinien, in research and pedagogy: A history of quantum physics through its textbooks, edited by M. Badino and J. Navarro, Edition Open Access, Berlin, pp. 117-135, 2013.

Edelman, A., Arias, T. A., Smith, S. T. The geometry of algorithms with orthogonality constraints. SIAM journal on Matrix Analysis and Applications, 1998, 20(2): 303-353.

Francisco, J. B., Martínez, J. M., Martínez,L. Globally conver-

gent trust-region methods for self-consistent field electronic structure calculations. The Journal of chemical physics, 2004, 121(22): 10863-10878.

Feng, X., Chen, M., Wu, Y., et al. A fully explicit and unconditionally energy-stable scheme for Peng-Robinson VT flash calculation based on dynamic modeling. Journal of Computational Physics, 2022, 463: 111275.

Francis, J. G. The QR transformation a unitary analogue to the LR transformation-Part 1. The Computer Journal, 1961, 4(3): 265-271.

Francis, J. G. The QR transformation-part 2. The Computer Journal, 1962, 4(4): 332-345.

Geltner, P. B. General Rayleigh quotient iteration. SIAM Journal on Numerical Analysis, 1981, 18(5): 839-843.

Greeley, J., Mavrikakis, M. Alloy catalysts designed from first principles. Nature materials, 2004, 3(11): 810-815.

Griffiths, D. J., Schroeter, D. F. Introduction to quantum mechanics. Cambridge, England, Cambridge University Press, 2018.

Gasiorowicz, S. Quantum physics. New Jersey, USA, John Wiley & Son Ltd, 2003.

Golebiewski, A. L. O. J. Z. Y., Taylor, H. S. Quantum theory of atoms and molecules. Annual Review of Physical Chemistry, 1967, 18(1): 353-408.

Gupta, A. K., Verma, K., Niazi, K. R. Robust coordinated control for damping low frequency oscillations in high wind penetration power system. International Transactions on Electrical Energy Systems, 2019, 29(5): e12006.

Gomer, R. Approaches to the theory of chemisorption. Accounts of Chemical Research, 1975, 8(12): 420-427.

Hammer, B., Norskov, J. K. Why gold is the noblest of all the metals. Nature, 1995, 376(6537): 238-240.

Helmberg, C., Rendl, F. A spectral bundle method for semidefinite programming. SIAM Journal on Optimization, 2000, 10(3): 673-696.

Harne, R. L. The concurrent suppression of, and energy harvesting from, surface vibrations: Experimental investigations. In Active and Passive Smart Structures and Integrated Systems. SPIE, 2012, 8341: 493-504.

Huang, L., Qiu, D., Xie, F., et al. Modeling and stability analysis of a single-phase two-stage grid-connected photovoltaic system. Energies, 2017, 10(12): 2176.

Huang, B., Kwon, H., Ko, J., et al. Density functional theory study for the enhanced sulfur tolerance of Ni catalysts by surface alloying. Applied Surface Science, 2018, 429: 87-94.

Huzaifa, M., Shafiq, M., Ali, N., et al. Au-decorated $Ti_3C_2$ MXene sensor for enhanced detection of gaseous toxins (CO, $COCl_2$, $H_2S$, $NH_3$, $NO_2$): A DFT study. ACS omega, 2024, 10(1): 1562-1570.

Hohenberg, P., Kohn, W. Inhomogeneous electron gas. Physical Review, 1964, 136(3B): B864-B971.

He, W. Prabhu, N. Jacobi decomposition and eigenvalues of symmetric matrices, in discrete and computational geometry: The Goodman-Pollack Festschrift, edited by B. Aronov, S. Basu, J. Pach & M. Sharir, Springer Berlin Heidelberg, Berlin, Heidelberg, pp. 527-550, 2003.

Jackiw, R. Intermediate quantum mechanics. Boca Raton, USA, CRC Press, 2018.

Jiang, B., Dai, Y. A framework of constraint preserving update schemes for optimization on Stiefel manifold. Mathematical Programming, 2015, 153(2): 535-575.

Kohn, W., Sham, L. J. Self-consistent equations including exchange and correlation effects. Physical Review, 1965, 140(4A): A1133-A1138.

Kerdphol, T., Rahman, F. S., Watanabe, M., et al. Small-signal analysis of multiple virtual synchronous machines to enhance frequency stability of grid-connected high renewables. IET Generation, Transmission & Distribution, 2021, 15(8): 1273-1289.

Khazanov, V. B., Kublanovskaya, V. N. Spectral problems for matrix pencils: Methods and algorithms II. Russian Journal of Numerical Analysis and Mathematical Modelling, 1988, 3(6): 467-486.

Kressner, D. A block Newton method for nonlinear eigenvalue problems. Numerische Mathematik, 2009, 114(2): 355-372.

Kublanovskaya, V. N. On an approach to the solution of the generalized latent value problem for $\lambda$-matrices. SIAM Journal on Numerical Analysis, 1970, 7(4): 532-537.

Kashiwagi, M. A numerical method for eigensolution of locally modified systems based on the inverse power method. Finite Elements in Analysis and Design, 2009, 45(2): 113-120.

Kaniel, S. Estimates for some computational techniques in linear algebra. Mathematics of Computation, 1966, 20(95): 369-378.

Liu, X., Oishi, S. I. Guaranteed high-precision estimation for $P_0$ interpolation constants on triangular finite elements. Japan Journal of Industrial and Applied Mathematics, 2013, 30(3): 635-652.

Liu, X., Oishi, S. I. Verified eigenvalue evaluation for the Laplacian over polygonal domains of arbitrary shape. SIAM Journal on Numerical Analysis, 2013a, 51(3): 1634-1654.

Liu, X., Kikuchi, F. Analysis and estimation of error constants for $P_0$ and $P_1$ interpolations over triangular finite elements. Journal of Mathematical Sciences (Tokyo), 2010, 17(1): 27-78.

Li, P., Wei, H., Li, B., et al. Eigenvalue-optimisation-based optimal power flow with small-signal stability constraints. IET Generation, Transmission & Distribution, 2013, 7(5): 440-450.

Lima, E. E. S. A sensitivity analysis of eigenstructures [in power system dynamic stability]. IEEE transactions on power systems, 2002, 12(3): 1393-1399.

Li, Q., Li, Y., Zeng, W. Preparation and application of 2D MXene-based gas sensors: A review. Chemosensors, 2021, 9(8): 225.

Li, M., Wang, X. Two-dimensional th-BCP monolayer as a superior sensor for detecting toxic gases: A first-principles study. ACS Applied Electronic Materials, 2024, 6(9): 6440-6449.

Lü, B., Chen, G, Zhou, W., et al. A density functional theory study on influence of 3d alloying elements on electrochemical properties of cobalt-base alloys. Computational

materials science, 2013, 68: 206-211.
Liu, X., Wang, X., Wen, Z., et al. On the convergence of the self-consistent field iteration in Kohn–Sham density functional theory. SIAM Journal on Matrix Analysis and Applications, 2014, 35(2): 546-558.
Liu, X., Wen, Z., Wang, X., et al. On the analysis of the discretized Kohn-Sham density functional theory. SIAM Journal on Numerical Analysis, 2015, 53(4): 1758-1785.
Montemore, M. M., Medlin, J. W. A unified picture of adsorption on transition metals through different atoms. Journal of the American Chemical Society, 2014, 136(26): 9272-9275.
Norsko, J. K. Chemisorption on metal surfaces. Reports on Progress in Physics, 1990, 53(10): 1253.
Nørskov, J. K., Rossmeisl, J., Logadottir, A., et al. Origin of the overpotential for oxygen reduction at a fuel-cell cathode. The Journal of Physical Chemistry B, 2004, 108(46): 17886-17892.
Nielsen, M. A., Chuang, I. L. Quantum computation and quantum information. Cambridge, UK, Cambridge University Press, 2010.
Nair, R. G. S., Nair, A. K. N., Yan, B., et al. Doped hexa-perihexabenzocoronene as anode materials for lithium-and magnesium-ion batteries. Physical Chemistry Chemical Physics, 2025, 27(1): 218-231.
Nair, R. G. S., Nair, A. K. N., Sun, S. Adsorption of drugs on $B_{12}N_{12}$ and $Al_{12}N_{12}$ nanocages. RSC advances, 2024, 14(43): 31756-31767.
Nair, R. G. S., Nair, A. K. N., Sun, S. Density functional theory study of doped coronene and circumcoronene as anode materials in lithium-ion batteries. Scientific Reports, 2024a, 14(1): 15220.
Nair, R. G. S., Nair, A. K. N., Sun, S. Adsorption of gases on $B_{12}N_{12}$ and $Al_{12}N_{12}$ nanocages. New Journal of Chemistry, 2024b, 48(18): 8093-8105.
Nair, R. G. S., Nair, A. K. N., Sun, S. Adsorption of hazardous gases on Cyclo [18] carbon and its analogues. Journal of Molecular Liquids, 2023, 389: 122923.
Nair, R. G. S., Nair, A. K. N., Sun, S. Adsorption of Gases on Fullerene-like $X_{12}Y_{12}$ (X= Be, Mg, Ca, B, Al, Ga, C; Y= C, Si, N, P, O) Nanocages. Energy & Fuels, 2023a, 37(18): 14053-14063.
Neumaier, A. Residual inverse iteration for the nonlinear eigenvalue problem. SIAM journal on numerical analysis, 1985, 22(5): 914-923.
Pacchioni, G. Electronic interactions and charge transfers of metal atoms and clusters on oxide surfaces. Physical Chemistry Chemical Physics, 2013, 15(6): 1737-1757.
Parlett, B. N. Misconvergence in the Lanczos algorithm, in Reliable Numerical Computation, edited by M. G. Cox and S. Hammarling, Clarendon Press, Oxford, UK, pp. 7-24, 1990.
Patra, C., Guna, V. K., Chakraborty, S., et al. Advances in 2D transition metal Ddichalcogenide-based gas sensors. ACS sensors, 2025, 10(9): 6347-6379.
Quarteroni, A., Valli, A. Numerical approximation of partial differential equations. Berlin, Germany, Springer, 2008.
Ren, M., Guo, X., Huang, S. Coordination-tuned Fe single-atom catalyst for efficient CO2 electroreduction: The power of B atom. Chemical Engineering Journal, 2022, 433: 134270.
Schilling, N., Froyland, G., Junge, O. Higher-order finite element approximation of the dynamic laplacian. ESAIM: Mathematical Modelling and Numerical Analysis, 2020, 54(5): 1777-1795.
Schwarzendahl, S. M., Neubauer, M., Wallaschek, J. Optimization of a passive piezoelectric damper for a viscously damped main system. Society of Photo-Optical Instrumentation Engineers, 2012, 8341: 68-77.
Schrödinger, E. An undulatory theory of the mechanics of atoms and molecules. Physical review, 1926, 28(6): 1049-1070.
Sherrill, C. D., Schaefer III, H. F. The configuration interaction method: Advances in highly correlated approaches. Advances in quantum chemistry. Academic Press, 1999, 34: 143-269.
Shen, J., Xu, J., Yang, J. A new class of efficient and robust energy stable schemes for gradient flows. SIAM Review, 2019, 61(3): 474-506.
Shen, L., Xu, Z., Lin, P., et al. An energy stable $C^0$ finite element scheme for a phase-field model of vesicle motion and deformation. SIAM Journal on Scientific Computing, 2022, 44(1): B122-B145.
Sleijpen, G. L., Booten, A. G., Fokkema, D. R., et al. Jacobi-Davidson type methods for generalized eigenproblems and polynomial eigenproblems. BIT Numerical Mathematics, 1996, 36(3): 595-633.
Unger, H. Nichtlineare behandlung von eigenwertaufgaben. Zeitschrift Angewandte Mathematik und Mechanik, 1950, 30(8-9): 281-282.
Van Vleck, J. H. The theory of electric and magnetic susceptibilities. Oxford, UK, Oxford University Press, 1932.
Voss, H. An Arnoldi method for nonlinear eigenvalue problems. BIT numerical mathematics, 2004, 44(2): 387-401.
Walter, M. G., Warren, E. L., McKone, J. R., et al. Solar water splitting cells. Chemical reviews, 2010, 110(11): 6446-6473.
Wang, F., Su, Q., Zhang, X., et al. Spin-state regulation of single-atom catalysts: From quantum mechanisms to multidimensional dynamic regulation strategies. Advanced Functional Materials, 2025: e18600.
Wang, X., Chen, H., Kou, J., et al. An unconditionally energy-stable and orthonormality-preserving iterative scheme for the Kohn-Sham gradient flow based model. Journal of Computational Physics, 2024, 498: 112670.
Yang, X., Ju, L. Efficient linear schemes with unconditional energy stability for the phase field elastic bending energy model. Computer Methods in Applied Mechanics and Engineering, 2017, 315: 691-712.
Zheng, M., Li, S., Su, Y., et al. Catalytic properties of near-surface alloy of transition metal in aluminum: A density functional theory study of structural and electronic properties. The Journal of Physical Chemistry C, 2013, 117(47): 25077-25089.
Zhou, A. An analysis of finite-dimensional approximations for the ground state solution of Bose-Einstein condensates. Nonlinearity, 2003, 17(2): 541.